Geophysical Journal International

Geophys. J. Int. (2011) **187,** 1250–1258 doi: 10.1111/j.1365-246X.2011.05224.x

Detecting uniaxial single domain grains with a modified IRM technique

R. Mitra, L. Tauxe and J. S. Gee

Scripps Institution of Oceanography, University of California, San Diego, 9500 Gilman Drive, La Jolla, CA 92093-0220, USA. E-mail: rmitra@ucsd.edu

Accepted 2011 September 7. Received 2011 August 25; in original form 2011 February 18

SUMMARY

Mid-ocean ridge basalt (MORB) specimens have often been found to have high ratios of saturation remanence to saturation magnetization (M_{rs}/M_s). This has been attributed either to dominant cubic anisotropy or to insufficient saturating field leading to overestimation of M_{rs}/M_s of a dominantly uniaxial single domain (USD) assemblage. To resolve this debate, we develop an independent technique to detect USD assemblages. The experimental protocol involves subjecting the specimen to bidirectional impulse fields at each step. The experiment is similar to the conventional isothermal remanent magnetization (IRM) acquisition experiment but the field is applied twice, in antiparallel directions. We define a new parameter, IRAT, as the ratio of the remanences at each field step and show it to have characteristic behaviour for the two assemblages; IRAT ∼1 at all field steps for USD and <1 with a strong field dependence for multi-axial single domain (MSD) grains. We verified the theoretical predictions experimentally with representative USD and MSD specimens. Experiments with MORBs gave low IRATs for specimens having high M_{rs}/M_s. This argues for a dominant MSD assemblage in the MORBs, possibly cubic in nature. Although undersaturation of the samples can indeed be a contributing factor to the exceptionally high M_{rs}/M_s, this study shows that the nature of the assemblage cannot be dominantly USD.

Key words: Magnetic fabrics and anisotropy; Magnetic mineralogy and petrology; Rock and mineral magnetism; Mid-ocean ridge processes.

1 INTRODUCTION

The ratio of saturation remanence to saturation magnetization (M_{rs}/M_s) is commonly used to identify uniaxial single domain (USD) particles, although the interpretation is not always straightforward. For example, the M_{rs}/M_s for randomly distributed USD grains has a theoretical upper limit of 0.5 (Stoner & Wohlfarth 1948), but mixing of USD grains with finer superparamagnetic (SP) or coarser multidomain (MD) grains inevitably reduces this ratio (Day *et al.* 1977). Day *et al.* (1978) and, more recently, Gee & Kent (1995), noted exceptionally high M_{rs}/M_s ratios (>0.5 and as high as 0.67) in some mid-ocean ridge basalts (MORBs). Gee & Kent (1995) attributed this to the dominance of grains with cubic anisotropy (as opposed to uniaxial anisotropy), because the theoretical limit for single domain (SD) grains with cubic anisotropy is 0.83 ($K_1 > 0$) or 0.87 ($K_1 < 0$), where K_1 is the magnetocrystalline anisotropy (Joffe & Heuberger 1974). Fabian (2006) offered an alternative explanation, arguing that the samples were essentially uniaxial but not saturated leading to an underestimation of M_s, making the M_{rs}/M_s ratio <0.5. Using a saturating field as high as 7 T, he showed for a single specimen that M_{rs}/M_s could be brought down from 0.5 (measured at 1 T) to 0.39, thereby, obviating the need for cubic anisotropy. Although lowering of M_{rs}/M_s with increasing field would be an indication of sample undersaturation, the evidence it presents for uniaxial anisotropy is inconclusive. Gee & Kent (1995) measured hysteresis parameters of one specimen at a 5 T field. The resulting M_{rs}/M_s ratio dropped from 0.63 (measured at 1 T) to 0.49. However, the presence of abundant observable MD grains in this specimen suggests that a ratio of 0.49 is the result of mixing of a population with ratios much higher than 0.5 (hence not USD) with grains having much lower ratios (the MD grains).

The assumption of uniaxial anisotropy of titanomagnetites in MORBs, stems from the low K_1 compared to magnetoelastic anisotropy (K_λ). In titanomagnetites, with moderate to high Ti content, equant grains lacking significant shape anisotropy have been shown to be dominated by stress anisotropy, which is assumed to be uniaxial (Appel & Soffel 1984; Appel 1987). Sahu & Moskowitz (1995) showed that $K_\lambda > K_1$ for most temperatures in TM60, a titanomagnetite with 60 per cent mole fraction of ulvöspinel, an important constituent of MORBs. Although stress control of the dominant anisotropy is largely agreed upon, the assumption of its uniaxial nature is more of a mathematical simplification than an empirical observation (Dunlop & Özdemir 1997, p. 44). In light of such findings, an independent test for detecting USD grains could prove to be useful. In this paper, we propose such a test.

The magnetization acquired by a specimen at room temperature through the application of an impulse field is known as isothermal remanent magnetization (IRM). In SD grains, there are a finite number of directions in which the magnetic moment tends to reside in the absence of an external field. Because moments in these directions have the minimum magnetic energy, they are known as 'easy directions'. With the application of a sufficient field, the moment can attain enough energy to cross the energy barrier between adjacent easy directions. In such a situation, the moment jumps, suddenly and irreversibly, from one easy direction to another, closer to the direction of the field. In SD grains, the field strength required to flip the moments is a function of the angular relation between the field and the moment. Therefore, the bulk coercivity of an assemblage could change depending on the angular relationship between the field, the available easy directions and the distribution of magnetic moments.

An IRM acquisition experiment generally involves subjecting a specimen to a stepwise increasing field. Here, we explore a double IRM experiment (DIRM) in which each field step comprises applying the same field strength twice, but, in antiparallel directions. The remanence is measured after *each* field application. We define the IRM ratio (IRAT) as the ratio of the absolute remanences, second over the first, at every step. IRAT has distinctive signatures for USD grains as opposed to SD grains showing multi-axial anisotropy (MSD) and is useful in addressing the controversy regarding the cubic anisotropy (a form of MSD) of some MORBs as proposed by Gee & Kent (1995) and disputed by Fabian (2006).

USD grains have by definition two easy directions in which the moment has minimum energy in the absence of an applied field. The first application of an instantaneous field in a dominantly USD assemblage will flip moments in some grains towards the easy direction closer to the field. When the field is applied in the reverse direction the angular relationships between the field and the moments remain unchanged because the inherent uniaxial symmetry of the grains is symmetric with respect to a bidirectional field. For example, if a grain moment makes an angle of 120° with the field and the field is sufficient to overcome the energy barrier, the moment will flip to the only other easy direction, at an angle of 60° with the field. Now, when the field direction is reversed the moment again makes an angle of 120° with the field, hence, a second field of the same magnitude is sufficient to flip the moment back. This ensures that the bulk coercivity does not change in USD grains under a bidirectional application of a field and consequently IRAT remains very close to 1.

In the case of a dominantly MSD assemblage, the first application of the field would flip moments in some grains into easy directions closer to the field. However in this case, when the field is reversed, the coercivity changes because the easy directions do not necessarily maintain the same symmetry with the field. For example, let us consider a grain of haematite showing sixfold anisotropy in the basal plane. There are six easy directions, each 60° apart. The first application of a sufficiently high-field acting in the basal plane of a grain would cause a moment at an angle of 90° with the field to overcome the necessary energy barrier and flip to an easy direction closer to the field. This direction would be at an angle of 30° with the field. Now, when the field direction is reversed, the new angle between the field and the moment would be 150° and the field strength could be inadequate to flip back the moment.

In essence, any departure from uniaxial symmetry is likely to show a change in coercivity with changing field directions. In fact, it will be shown in the following sections that this anisotropy is enough to exhibit substantially 'higher' coercivities during the second application of the field. As a result, IRAT will be always >1 in MSD grains for fields less than saturation.

Wohlfarth (1958) was the first to derive a simple relationship between the forward and backward remanences and suggested that the lack of reciprocity of the two could be due to non-uniaxial anisotropy, particle interaction or domain state. He did not comment on the exact mechanism of how these apparently dissimilar properties would affect the result or the nature of their influence. Although non-uniaxiality of anisotropy has been cited as one of the reasons for the observed phenomenon, the other reasons seem to have been invoked more often to explain similar phenomenon. Tauxe *et al.* (1990) in an experiment similar to DIRM, observed a 'sawtooth' in a sample containing specular haematite and ascribed that to relict MD signature in SD grains. A similar propensity is sometimes observed in the interpretation of Henkel plots, where IRM acquisition and DC demagnetization are plotted against each other (Henkel 1964). Instead of alternating the field direction at each step as in the DIRM experiment, this entails exposure of the sample to successively higher fields in one direction and subsequent demagnetization by applying increasingly negative fields in the opposite. This type of plot has long been used to analyse the strength of particle interaction. Much like an Arai plot for a palaeointensity experiment, where sagging of the curve is often ascribed to MD grains, non-linearity in the Henkel plots are often used as an indicator of interacting SD grains. More recently though, attention has been drawn to the fact that multi-axial anisotropy can also cause Henkel plots to be curved, with the remanence during the IRM acquisition leg being greater than during the dc demagnetization leg; a result in keeping with our tenet (Geshev & Mikhov 1992; Garcia-Otero *et al.* 2000). Garcia-Otero *et al.* (2000) further showed that this curvature would be in a direction opposite to that observed due to particle interaction and warned that the combined effect of the two could yield a straight line in a Henkel plot leading to erroneous interpretation.

In this paper, we will use numerical models and experimental evidence to demonstrate the difference in response of USD and MSD grains to DIRM acquisition. We will be using USD magnetite and MSD haematite to be representative of the two categories. We will then use DIRM acquisition curves to address the issue of the dominant anisotropy in MORBs. We will provide strong evidence for the presence of multi-axial anisotropy in the high M_{rs}/M_s MORB samples.

2 THEORY

2.1 Energy calculations

The total energy of an SD grain, assuming only coherent rotations of moments, is the sum of the anisotropy energy (E_{anis}) and the magnetostatic energy (E_{ms}) due to the external field. An SD grain showing n-fold anisotropy has n easy directions, where the total free energy density E_{tot} (energy per unit volume) is minimum. E_{tot} is given by

$$E_{tot} = E_{anis} + E_{ms} = K \sin^2\left(\frac{n}{2}\theta\right) - M_s B_{eff} \cos(\theta - \phi), \qquad (1)$$

where K is the anisotropy constant (e.g. K_1, K_u or K_λ), M_s is the saturation magnetization, B_{eff} is the effective field, θ the angle between the moment and the easy direction, and ϕ is the angle between the easy direction and B (Dunlop 1971).

For any grain in the absence of a field, the total energy per unit volume is equal to the anisotropy energy. With the application of an external field, the contribution of the magnetostatic energy rises. Using eq. (1) we can plot the energy profiles of a single grain of

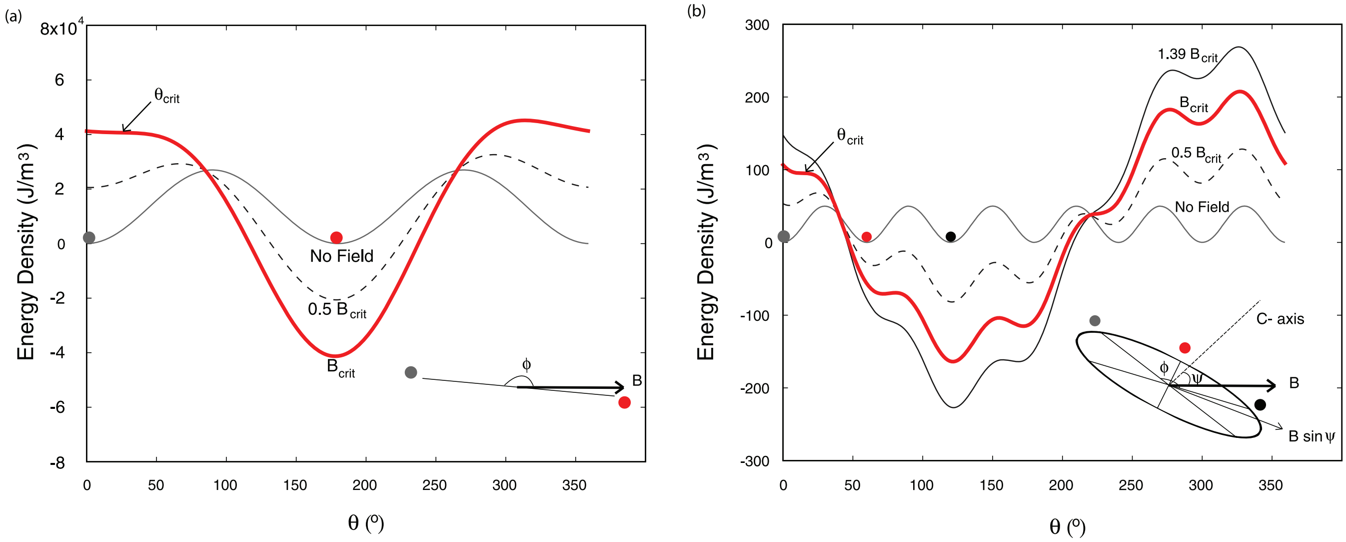

Figure 1. Energy density for $\theta = [0, 360]$ in (a) magnetite grains with $\phi = 175°$ and (b) haematite grains with $\phi = 130°$. Insets show the corresponding grains with easy directions (thin line) and field direction (thick). In (b) the *c*-axis is orthogonal to the plane containing easy directions. (a) In absence of a field the energy profile (grey) shows two energy minima (easy directions). For a field $0.5B_{\mathrm{crit}}$, the profile changes (dashed line), but the moment (grey dot) cannot flip to the other easy direction. Only when $B_{\mathrm{eff}} \geq B_{\mathrm{crit}}$, can the moment overcome the energy barrier and flip to a position 180° apart (red dot). (b) Without any field, the energy profile (grey) shows six energy minima (easy directions). As in the USD case, at any field less than B_{crit}, the energy profile changes but the moment (grey dot) cannot overcome the energy barrier. At B_{crit}, the moment flips instantaneously to an adjacent easy axis 60° apart (red dot). If the field was even higher ($1.39B_{\mathrm{crit}}$ for this particular grain), then the moment would have had its least energy configuration at an easy axis 120° (black dot) apart. Calculations are based on values used in text. See fig. 2 in Dunlop (1971) for additional graphs showing dependence of B_{crit} with ϕ for the two cases.

magnetite, having $n = 2$ easy directions (uniaxial), and a haematite grain, having $n = 6$ easy directions in the basal plane (multi-axial; Figs 1a and b, respectively). It is to be noted that haematite shows a dominant sixfold basal plane anisotropy only between the Morin transition ($\sim -10\,°$C) and the Néel temperature ($\sim 675\,°$C) (Besser *et al.* 1967). Below the Morin transition the moments are not constrained to lie in the basal plane, showing a pronounced uniaxiality along the *c*-axis instead.

In Fig. 1, the energy minima in the solid grey curves (no field) represent the easy directions. As we apply a field, the energy-density curves change. A small applied field moves the curves to the dashed lines but it is not large enough to remove barriers entirely from between the easy directions and the moment may stay trapped in the local energy minimum (grey dot). At a critical field value, B_{crit}, however, the curve changes to the heavy (red) line and the energy barrier is removed; the moment is able to flip to the adjacent energy minimum and remains there when the field is switched off (red dot on grey lines). The value of θ at B_{crit} is the critical angle, θ_{crit}. It is worth mentioning at this stage that the moment flips instantaneously from one direction to the other, hence, θ_{crit} is more of a mathematical construct than a physical quantity. Also, it is noteworthy that B_{eff} is the effective field. So for uniaxial magnetite, when the moment is free to rotate in any direction under the influence of the field, B_{eff} equals the applied field (B). However for a grain where the moments are constrained to lie in a particular plane, as in haematite, only the basal plane component, that is, $B\sin\psi$ makes up B_{eff} (Fig. 1, insets).

The condition for flipping is to remove the energy barrier (e.g. the humps between the grey and red dots in Fig. 1). This can be mathematically expressed in terms of the derivatives of the energy density curves when the first and second derivatives are both zero, that is, $\mathrm{d}E/\mathrm{d}\theta = \mathrm{d}^2E/\mathrm{d}\theta^2 = 0$. Solving for θ and B_{crit}, we get

$$\tan(n\theta_{\mathrm{crit}}) = n\tan(\theta_{\mathrm{crit}} - \phi), \tag{2}$$

and

$$B_{\mathrm{crit}} = -\frac{nK}{2M_{\mathrm{s}}}\frac{\sin(n\theta_{\mathrm{crit}})}{\sin(\theta_{\mathrm{crit}} - \phi)}. \tag{3}$$

The flipping condition is met when $B_{\mathrm{eff}} \geq B_{\mathrm{crit}}$.

2.2 Numerical simulation

To simulate DIRM as a function of applied field, we start with an assemblage of magnetic grains with randomly oriented moment directions along randomly oriented easy axes. A large number of grains in the simulation ensures a low initial remanence, reflecting a completely demagnetized state. We used 20 000 grains for our simulations, which gave an initial remanence of $\sim$1 per cent of saturation remanence. Increasing the number of grains gives even lower initial remanence but also increases the total runtime without significantly affecting the result. This is also more representative of our experimental conditions where we use the natural remanence (NRM) as the initial state. This is a fair approximation as long as the NRM is significantly lower than the IRM. We will discuss this in greater detail in Section 4.

We assumed shape-dominated uniaxial anisotropy in magnetite and used $M_{\mathrm{s}} = 480\,\mathrm{K\,Am^{-1}}$ for simulating an USD assemblage (Tauxe 2010, p. 68). A uniform prolate grain shape with axial ratio, $c/a = 1.9$, translates to a uniaxial anisotropy constant K_{u} of $27\,\mathrm{K\,Jm^{-3}}$. For simulating MSD grains, we used haematite, which has a sixfold basal plane anisotropy. A range from 10 to $100\,\mathrm{J\,m^{-3}}$ is suggested for magnetocrystalline anisotropy in haematite (Dunlop & Özdemir 1997). For the purpose of this simulation, we chose a value of $50\,\mathrm{J\,m^{-3}}$, noting that the results do not depend critically on the precise value. We used $M_{\mathrm{s}} = 2.1\,\mathrm{K\,Am^{-1}}$ for haematite (Tauxe 2010). An iterative routine of increasing field steps, with each field step comprising a $+B$ and $-B$ simulated DIRM acquisition. For each grain, the critical field, B_{crit}, for the moment to jump to the adjacent easy direction closer to the applied field B was calculated

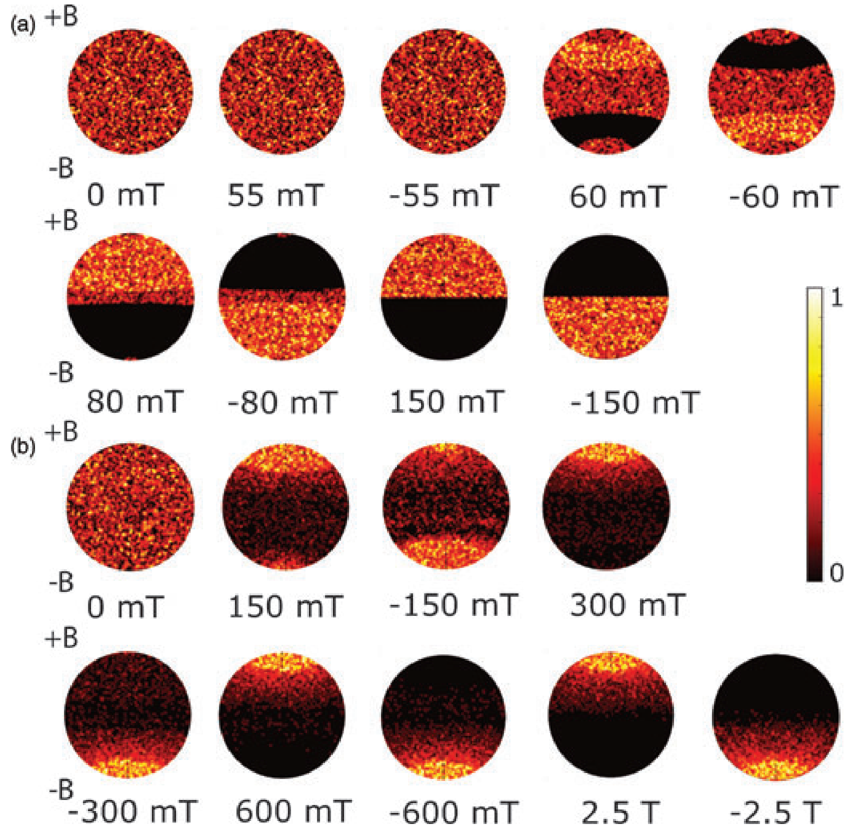

Figure 2. Kamb plots showing density of moments in response to different field steps for (a) USD magnetite and (b) MSD haematite. Only absolute value of inclinations were considered and the density was normalized by the maximum density of moments for that particular field step. Therefore, similar colours from different plots do not signify similar density.

using eqs (2) and (3). For those grains in which B_{crit} was found to be less than B_{eff}, the moments were transferred to the easy directions closer to the field direction. For USD grains this is a single-step process for each B, because the moments can reside only in two directions. For MSD grains, this can be a multistep process depending on the strength of the applied field (Fig. 1b). The simulations yielded M_{rs}/M_s values of 0.5 and 0.94 for the uniaxial and triaxial cases, respectively. For the latter, the moment was constrained to lie in the basal plane.

In USD assemblages, reversing the field direction flips the moments from one direction to the opposite. As a result, there is no difference in net magnetization of the bulk distribution of moments at any B or $-B$ (Fig. 2a). At ± 60 mT, all moments, having the lowest coercivity, flip towards the field. Since we have assumed that all grains have the same size and shape, coercivity is strictly a function of ϕ. Hence, the moments that are flipped to the antipodal easy directions at any particular field, all lie on a cone around the field direction. This is manifested in the form of small circles in Fig. 2. The number of such circles increases (note the expanding dark patch in Fig. 2a from 60 to 150 mT) with increasing field until saturation, at which all the moments are confined to one hemisphere. At each field step, the distribution of moments is symmetric with respect to the field direction (e.g. at 60 and -60 mT), thereby, giving the same net remanence. As a result, the remanence acquisition curve is smooth and IRAT is $\sim$1 at all field steps (Fig. 3a). This is strictly true only for a completely demagnetized initial state (solid circles in inset to Fig. 3a). For a simulated sample with an initial remanence of $\sim$2 per cent of the saturation remanence (either parallel to or antiparallel to the first field direction), the ratio changes to a value more (small open circles in inset to Fig. 3a) or less than unity (small open squares in inset to Fig. 3a) approaching unity as the field increases from 60 to 100 mT. The ratio is either more or less than unity, when the NRM is parallel or antiparallel to the direction of the first-applied field. If the NRM is $\sim$5 per cent of saturation remanence, IRAT shows at most $\sim$10 per cent departure from unity (larger symbols in the inset to Fig. 3a). As NRM of natural samples is usually weak and is unlikely to be 5 per cent of saturation remanence, IRAT is expected to be within 10 per cent of unity in natural USD assemblages.

In MSD assemblages, coercivity changes as a function of the history of fields applied. This effect is especially marked at low fields. Fig. 2(b) shows that at 150 mT, the concentration of moments is near the field azimuth in the $+B$ hemisphere (direction of the first-field application and top of diagrams). When the field is reversed, there are distinct concentrations in both the hemispheres. This is because at -150 mT, the field is not strong enough to sweep away the moments that are already at a high obtuse angle, ϕ, to the -150 mT field direction owing to prior application of the $+150$ mT field. Therefore, a fraction of the moments from the 150 mT step do not flip and effectively cancel out the contribution from the concentration of moments in the $-B$ hemisphere after the -150 mT step. This gives rise to a pronounced sawtooth pattern in the DIRM acquisition plot (Fig. 3b). IRAT increases from 0.06 at 100 mT to 0.99 at 600 mT (Fig. 3b, inset). At higher fields, the field strength compensates partially for this effect. Thus, the moment distribution at ± 600 mT and higher fields are almost mirror images of each other, whereas those at ± 150 mT are markedly different (Fig. 2b).

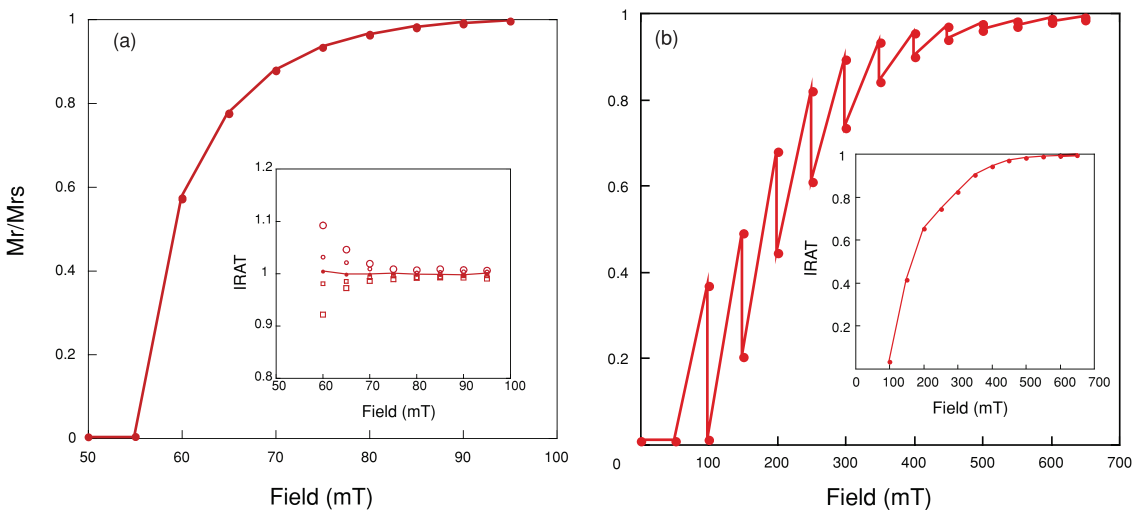

Figure 3. DIRM acquisition curves for (a) USD magnetite. Inset shows IRAT for the corresponding field steps (solid line). Open circles/squares show IRAT for a 2 per cent (small symbols), 5 per cent (big symbols) NRM at 0°/180° to the initial field direction and (b) MSD haematite. Inset shows IRAT for the corresponding field steps. Remanence (M_r) is normalized by saturation remanence (M_{rs}).

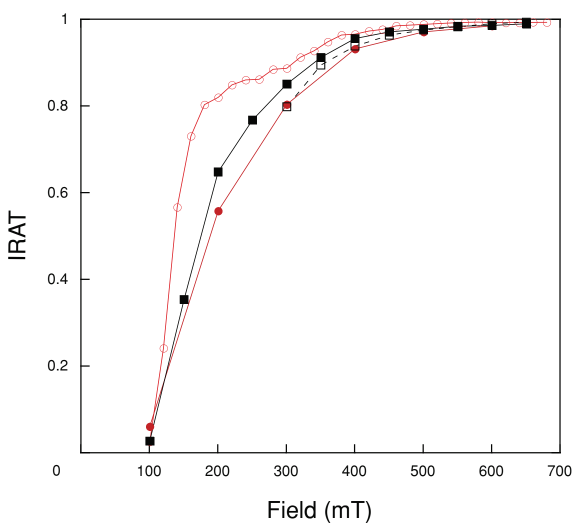

Figure 4. IRAT as a function of field spacing and initial field in MSD grains. Circles show IRAT for field spacing of 20 mT (open red) and 100 mT (closed red). Squares show IRAT for an initial field of 50 mT (closed black) and 300 mT (open black).

These results have a bearing on alternating-field (AF) demagnetization. In AF demagnetization, a specimen is exposed to an AF that has a sinusoidal waveform. The field decreases linearly with time and traps comparable number of moments along opposite directions. This gives rise to a net-zero moment. Although our experiment is very different from an AF demagnetization, both are affected by the coercivity spectrum in an analogous manner. The linearly reducing AF can trap disproportionately, more moments along one direction giving rise to strong remanence. This could explain spurious ARMs sometimes observed in the laboratory, even when no detectable field bias or bad waveform was present.

The sawtooth is more pronounced at low fields and is also sensitive to the spacing of the field steps (Fig. 4). For example, at 200 mT, IRAT varied between 0.56 and 0.81 depending on the choice of field steps, which in these experiments ranged between 20 and 100 mT. Increasing the number of field steps lowers the difference in coercivity of the successive field steps. The intermediary field steps help to 'soften' the coercivity by churning the moment directions multiple times. The choice of the initial field step has a similar, albeit less pronounced, effect on IRAT. For example, at 300 mT, IRAT varies from 0.79 to 0.85 for initial fields of 50 and 300 mT, respectively, with the same field step spacing of 50 mT. These results, together with the variability of grain size and coercivity of natural rocks, suggest that the absolute IRM values from very different samples might not be comparable. Despite these caveats, the property of IRAT, being close to unity and showing little change with field step for USD grains, can be used to distinguish between dominantly USD and dominantly MSD assemblages.

3 EXPERIMENTAL EVIDENCE

The theory and modelling in the preceding sections predict that USD and MSD assemblages will behave differently in a DIRM acquisition experiment. To test this experimentally, we investigate two sample types: the Tiva Canyon tuff and a specularite–haematite sample from the Dhok Pathan formation in Pakistan.

The Tiva Canyon tuff has been proposed as a standard USD material (Carter-Stiglitz *et al.* 2006). Hysteresis loops (Fig. 5a) look like classic SD loops predicted by Stoner & Wohlfarth (1948). First-order reversal curve (FORC) distributions (Pike *et al.* 1999; Roberts *et al.* 2000) show typical non-interacting SD behaviour with closed contours parallel to the B_c axis, a density peak near 40 mT and a small spread along B_u (Fig. 6a).

Tauxe *et al.* (1990) characterized the haematite found in the Dhok Pathan formation of the Siwalik Group in Pakistan as either specular or pigmentary types. The sedimentary sequence, comprising grey to red siltstones, have varying proportions of these phases. In this study, we chose one of the grey specimens that was reported to have primarily specular haematite with low coercivity.

The experimental protocol involved subjecting a specimen to an impulse DC field (B) in a pulse magnetizer and measuring the remanence. The specimen was then placed in the opposite direction in the pulse magnetizer and subjected to the same field (now, $-$B) and the remanence was remeasured. This was repeated at successively higher fields.

In a DIRM acquisition plot, no substantial sawtooth was observable in the Tiva Canyon tuff and the lowest IRAT was as high as

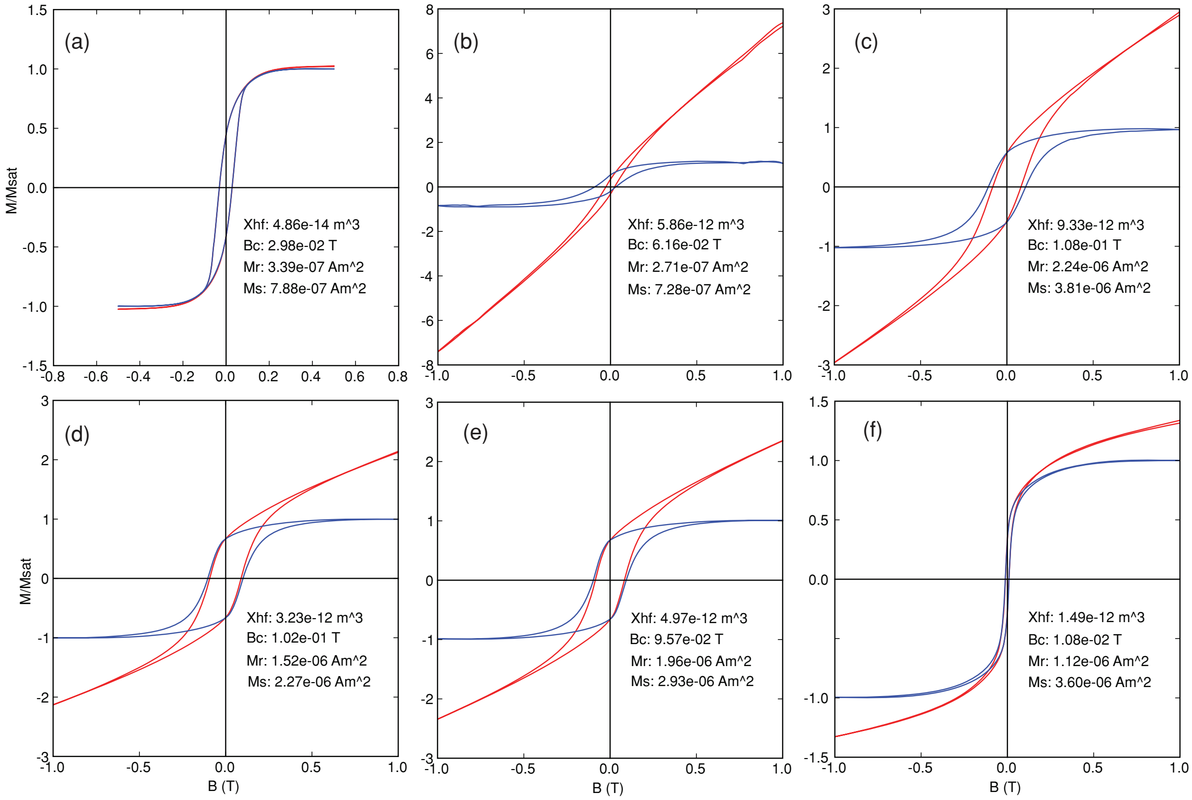

Figure 5. Representative hysteresis behaviour for (a) Tiva Canyon tuff (b–f) Ph93-1 at 1, 3, 5, 7 and 30 mm from the glassy margin.

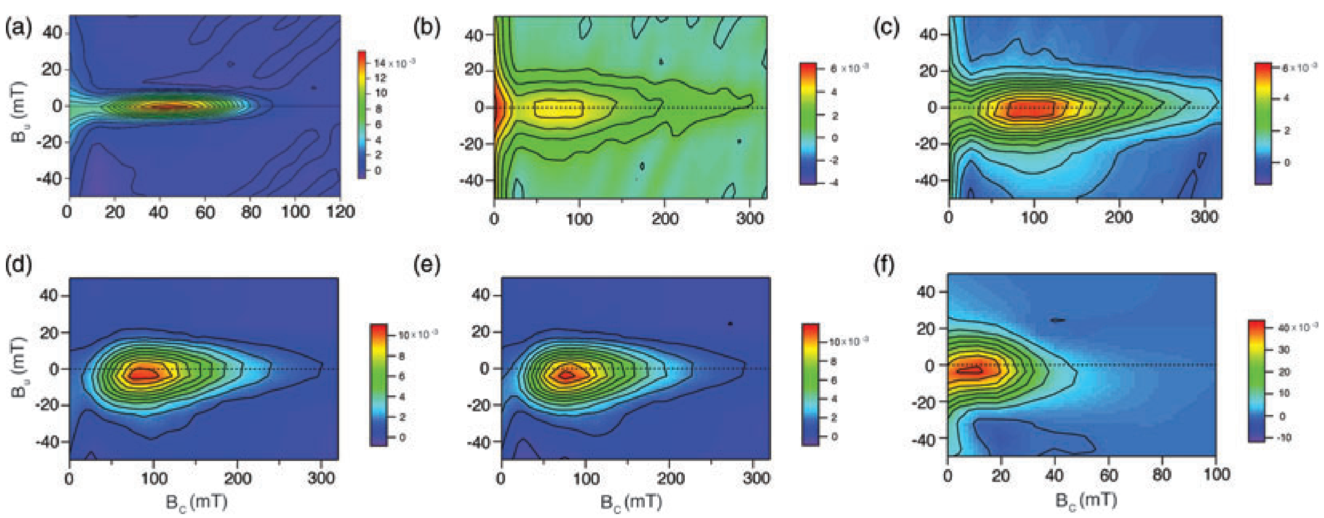

Figure 6. FORC distributions for (a) Tiva Canyon tuff (b–f) Ph93-1 at 1, 3, 5, 7 and 30 mm from the glassy margin. FORC distributions were prepared with the software described in Harrison *et al.* (2008).

0.94 at 30 mT (Fig. 7a). Specularite–haematite, on the other hand, showed a substantial sawtooth with IRAT increasing gradually from 0.57 at 50 mT to 0.97 at 600 mT (Fig. 7b). As predicted from theory: (1) the lowest IRAT was observed at the lowest field, (2) USD and MSD assemblages have distinct DIRM signatures and (3) IRAT at the first-field step shows the most difference for USD and MSD assemblages and can be used to effectively discriminate between the two. In the following section, we will be using the first-field IRAT to understand the dominant source of magnetic anisotropy energy in the MORBs initially studied by Gee & Kent (1999).

4 NATURE OF ANISOTROPY ENERGY IN MORB SAMPLES

To investigate the nature of anisotropy in MORBs, we started with a 0.18 Ma sample (PH93-1) from the Phoenix expedition near 10°N on the East Pacific Rise (Batiza *et al.* 1996). Gee & Kent (1999) used specimens from this sample to show that magnetic granulometry varied as a function of the distance from the chilled margin. The M_{rs}/M_s ratios of some of the specimens were extremely high (>0.5).

For this study, we cut four slices of PH93-1 at ∼1–2 mm resolution parallel to the chilled margin for the outermost 1 cm.

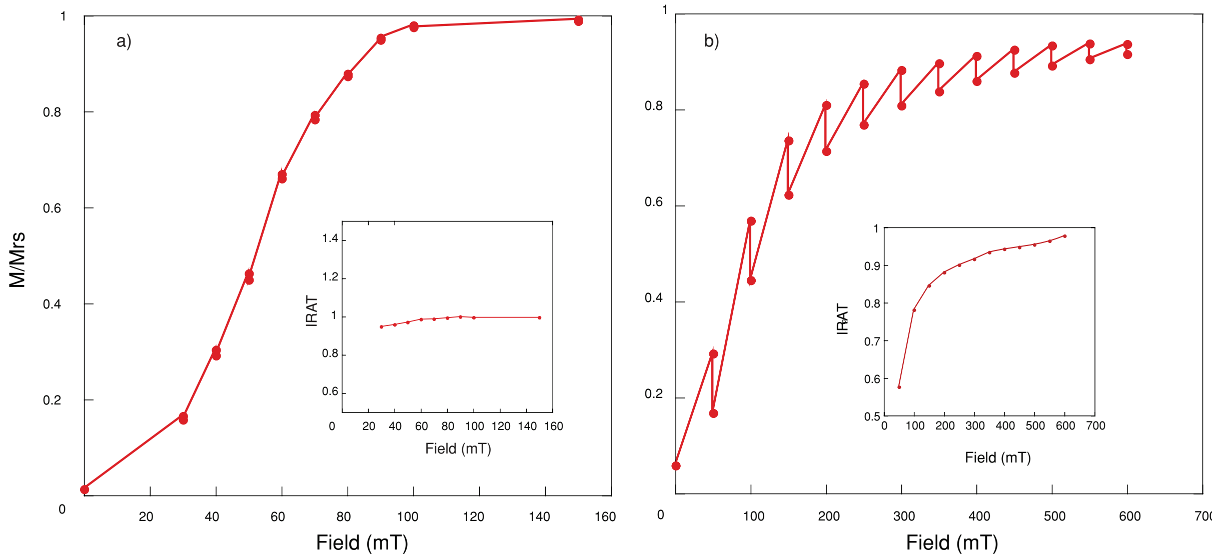

Figure 7. DIRM acquisition in natural samples. M_{rs} measured at 2.4 T. Inset shows corresponding IRATs. (a) Tiva Canyon tuff. (b) Dhok Pathan haematite.

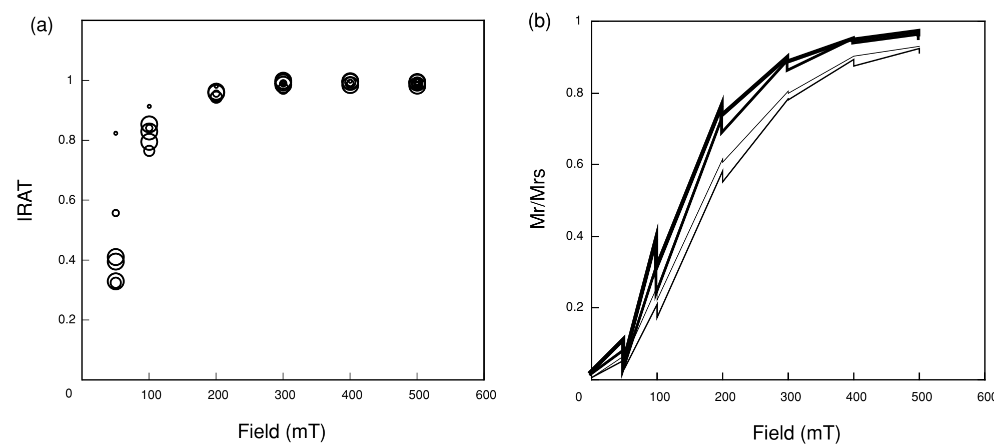

Figure 8. (a) IRAT as a function of field for PH93-1 specimens. Circle size represents distance from the margin, that is, 1(smallest circle), 3, 5 and 7 mm. (b) Corresponding DIRM acquisition in representative specimens. Line thickness increases with distance from the margin. Only one specimen shown from each zone.

Multiple specimens weighing between 20 and 100 mg were obtained by breaking apart each thin slice. The specimens were subjected to a complete DIRM acquisition experiment. Subsequently, FORCs were determined for all specimens. The slices had distinct hysteresis behaviour (Figs 5b–e) and derived FORC distributions (Figs 6b–e), consistent with the inferred increasing magnetic grain size away from the quenched margin. Peaks near $B_c = 0$ and FORC distribution contours parallel to B_u reflect a dominantly SP fraction (Fig. 6b). As we move away from the margin, the coercivity peak moves towards higher B_c values, consistent with an increasing SD fraction (Fig. 6c). For specimens ∼0.5–0.8 mm away from the glassy margin the contours close and the spread along B_u reduces, suggesting a dominantly SD contribution (Figs 6d and e). Further away, the contours open up again, but with higher coercivity peak than in Fig. 6(b), showing substantial MD contribution (Fig. 6f).

We subjected all specimens to the DIRM experiment (Fig. 8). DIRM acquisitions of the samples show IRAT increasing with field (Fig. 8). Specimens closest to the margin have the highest IRAT values (0.81 at 50 mT) and IRAT decreases with distance from the margin. At higher fields (200 mT), the difference in IRAT vanishes because the field strength overwhelms the difference in coercivity as the specimens approach saturation.

To further investigate the nature of the anisotropy energy we analysed two more approximately zero-age MORB samples; a pillow basalt (PH99-1) from 10°N on the East Pacific Rise (Batiza *et al.* 1996) and a ∼8-cm-thick sheet flow (MW86-5) from the southern East Pacific Rise (Sinton *et al.* 1991). The first centimetre of these samples were carefully sliced into chips measuring ∼1–2 mm in thickness. Each chip was further subdivided into 2–6 specimens measuring 20–100 mg. Three more specimens were sampled from the interior of the three basalts (>3 cm). A curtailed double-IRM protocol, involving just the initial step was carried out. The initial field was 50 mT for PH93-1 and 75 mT for the rest. Subsequently, hysteresis loops were determined and M_{rs}/M_s ratios were calculated using paramagnetic slope correction from 0.7 to 1 T.

To avoid high temperature alteration of the specimens, we avoided thermal demagnetization. Instead, the NRM was used as the initial state. The potential bias introduced, as a result, should be negligible as long as the IRM, after the first applied field, is substantially higher than the NRM. This would show that the potential bias due to existing NRM is negligible. For our purposes, we needed

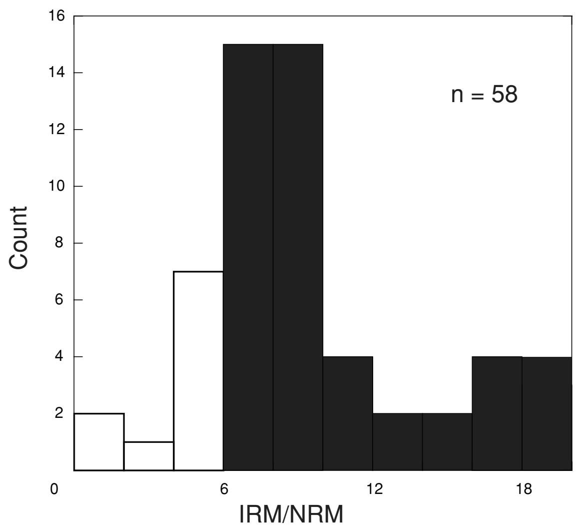

Figure 9. Histogram of the ratio of IRM at the first field step to NRM. Values 38.5 and 60 have been omitted from the figure. White bars denote samples which did not meet our selection criteria.

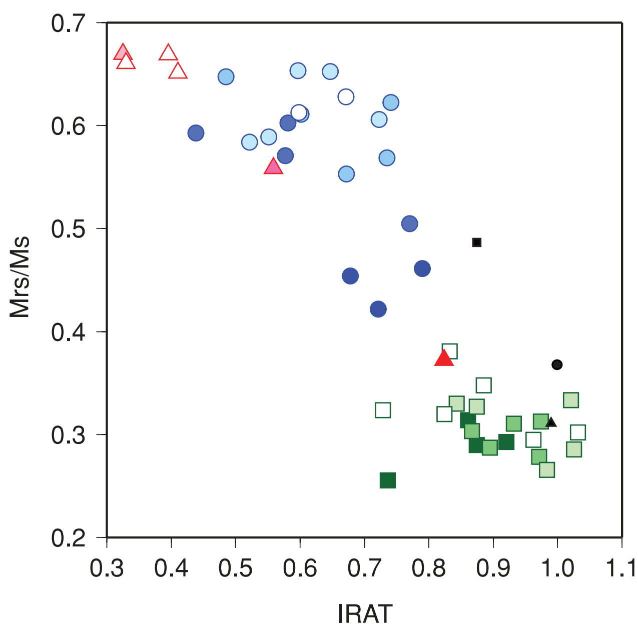

Figure 10. M_{rs}/M_s versus IRAT at the first field step for PH93-1 (red triangles, $n = 7$), PH99-1 (blue circles, $n = 20$) and MW86-5 (green squares, $n = 21$). Colour tones indicate distance from the chilled margin with deeper tones being closer to the margin and white symbols represent farthest (~1 cm) from the margin. Specimens lying >3 cm from the margin are shown with smaller black symbols.

a selection criterion, which would recognize specimens that were affected by the NRM bias. When IRM exceeded the NRM by a factor of 6 or more, it was assumed that the bias, due to such a low NRM, was negligible. 10 of the 58 samples did not meet this criteria and were excluded from this discussion (Fig. 9). IRAT data versus M_{rs}/M_s data for the remaining specimens are shown in Fig. 10 . Three specimens had IRATs slightly above one and although this is arguably due to an initial NRM bias (as shown in Fig. 3a, inset), the IRM was strong enough not to warrant an exclusion of these specimens.

We see a gradual transition from high M_{rs}/M_s, low-IRAT specimens to low M_{rs}/M_s, high-IRAT specimens. More importantly, specimens having M_{rs}/M_s above 0.5, all have IRAT values below 0.8 and sometimes as low as 0.3 (Fig. 10). Such low values of IRATs are consistent with our hypothesis of substantial MSD contribution in MORBs. The mostly glassy MW86-5 specimens, all cluster in a low M_{rs}/M_s, high-IRAT section of Fig. 10 (squares). On the other hand, pillow specimens, especially PH93-1(triangles), show a moderate dependence of IRAT with distance from the margin with higher IRAT in specimens closer to the margin. The high IRAT can be either due to a greater contribution of USD magnetite or an effect of SP fraction, as shown in Garcia-Otero *et al.* (2000). Specimens from the flow interiors have MD hysteresis behaviour (Fig. 5f) and the derived FORC distributions have open contours and low coercivity (Fig. 6f) showing dominant MD contribution. These specimens typically have a high IRAT values. Although a theoretical treatment of IRAT in MD grains is beyond the scope of this work, it is postulated that the mobile walls of the MD grains, being less coercive than the anisotropy of SD grains, are easier to re-organize under the influence of an external field, thereby, contributing to substantially higher IRATs, even at low fields.

An independent case for the presence of multi-axial anisotropy in MORBs has been presented by Lanci (2010), in which he used anisotropy of susceptibility to establish the presence of dominant cubic anisotropy. Another proposed mechanism for high M_{rs}/M_s as well as the high coercivity, as observed in these basalts, was the 3-D cross structure of Tauxe *et al.* (2002). These cross structures are composed of three parallelepipeds intersecting in three mutually orthogonal directions. Although reversals in magnetization in such complicated shapes show flower and vortex states and is not possible to model *sensu-stricto* within the framework discussed in this paper, the presence of more than one easy direction would arguably lower the IRAT. Hence, although it is possible that the anisotropy is indeed cubic, this work does not rule out more complicated possibilities.

5 CONCLUSIONS

(i) We define a new parameter IRAT (the ratio of two opposing low-field IRMs imparted in a double IRM-acquisition experiment) for differentiating between USD and MSD grains. With numerical simulation and experimental data, we show that, IRAT is ~1 for USD grains for all fields. For MSD grains, IRAT approaches 1 from lower values with increasing field.

(ii) We have shown that, in a system with dominant multi-axial anisotropy, coercivity varies with application of a field. At fields close to saturation, both USD and MSD grains have IRAT values of ~1. This suggests that, for samples where MSD grains may be present, experiments like anisotropy of isothermal remanence should be conducted at fields close to saturation, where the difference of remanences become negligible. Otherwise the experiments will always show a substantial anisotropy, even when there is none. Presence of MSD grains can impart strong remanences during AF demagnetization and can be a source of spurious ARMs, sometimes observed in the laboratory. On the other hand, parameters such as, HIRM and *S*-ratios, which are chiefly used as proxies for the relative amount of goethite/haematite as compared to softer minerals, like magnetite/maghemite, are unlikely to be affected much by this because of the large difference in coercivity between the two groups.

(iii) All our hysteresis parameters have been measured at 1 T maximum field. As noted earlier, Fabian showed that such a field might be underestimating the saturation magnetization which could potentially explain the high M_{rs}/M_s in some specimens. Despite that, our work shows, the specimens cannot have a dominant USD fraction.

(iv) If $K_\lambda > K_1$ for most MORBs then contrary to the popular assumption, stress anisotropy could be non-uniaxial.

ACKNOWLEDGMENTS

The authors gratefully acknowledge useful discussions with Luca Lanci and David Dunlop. This work was supported in part by NSF grant EAR1013192 to Lisa Tauxe. Reviews by two anonymous reviewers helped to improve the manuscript.

REFERENCES

Appel, E., 1987. Stress anisotropy in Ti-rich titanomagnetites, *Phys. Earth planet. Inter.,* **46**(1–3), 233–240.

Appel, E. & Soffel, H.C., 1984. Model for the domain state of Ti-rich titanomagnetites, *Geophys. Res. Lett.,* **11**(3), 189–192.

Batiza, R., Niu, Y.L., Karsten, J.L., Boger, W., Potts, E., Norby, L. & Butler, R., 1996. Steady and non-steady state magma chambers below the East Pacific Rise, *Geophys. Res. Lett.,* **23**(3), 221–224.

Besser, P.J., Morrish, A.H. & Searle, C.W., 1967. Magnetocrystalline anisotropy of pure and doped hematite, *Phys. Rev.,* **153**(2), 632–642.

Carter-Stiglitz, B., Solheid, P., Egli, R. & Chen, A., 2006. Tiva Canyon Tuff (II): near single domain standard reference material available, *IRM Quart.,* **16**(1), 9–11.

Day, R., Fuller, M. & Schmidt, V.A., 1977. Hysteresis properties of titanomagnetites–grain-size and compositional dependence, *Phys. Earth planet. Inter.,* **13**(4), 260–267.

Day, R., Halgedahl, S., Steiner, M., Kobayashi, K., Furuta, T., Ishii, T. & Faller, A., 1978. Magnetic properties of basalts from DSDP Leg, *Init. Rep. DSDP,* **49,** 781–791.

Dunlop, D.J., 1971. Magnetic properties of fine-particle hematite, *Ann. Geophys.,* **27**(3), 269–283.

Dunlop, D.J. & Özdemir, Ö., 1997. *Rock Magnetism: Fundamentals and Frontiers,* p. 44, Cambridge University Press, Cambridge.

Fabian, K., 2006. Approach to saturation analysis of hysteresis measurements in rock magnetism and evidence for stress dominated magnetic anisotropy in young mid-ocean ridge basalt, *Phys. Earth planet. Inter.,* **154**(3–4), 299–307, doi:10.1016/j.pepi.2005.06.016.

Garcia-Otero, J., Porto, M. & Rivas, J., 2000. Henkel plots of single-domain ferromagnetic particles, *J. app. Phys.,* **87**(10), 7376–7381.

Gee, J. & Kent, D.V., 1995. Magnetic hysteresis in young mid-ocean ridge basalts: dominant cubic anisotropy, *Geophys. Res. Lett.,* **22**(5), 551–554.

Gee, J. & Kent, D.V., 1999. Calibration of magnetic granulometric trends in oceanic basalts, *Earth planet. Sci. Lett.,* **170**(4), 377–390.

Geshev, J. & Mikhov, M., 1992. Remanence curves for a disordered system of 3-axial and 4-axial fine particles–Henkel-Type Plots, *J. Magn. Magn. Mat.,* **104,** 1569–1570.

Harrison, R.J. & Feinberg, J.M., 2008. FORCinel: an improved algorithm for calculating first-order reversal curve distributions using locally weighted regression smoothing, *Geochem. Geophys. Geosyst.,* **9**, Q05016, doi:2008GC001987.

Henkel, O., 1964. Remanenzverhalten und wechselwirkungen in hartmagnetischen teilchenkollektiven, *Phys. Stat. Sol.,* **7**(3), 919–929.

Joffe, I. & Heuberger, R., 1974. Hysteresis properties of distributions of cubic single-domain ferromagnetic particles, *Phil. Mag.,* **29**(5), 1051–1059.

Lanci, L., 2010. Detection of multi-axial magnetite by remanence effect on anisotropy of magnetic susceptibility, *Geophys. J. Int.,* **181**(3), 1362–1366, doi:10.1111/j.1365-246X.2010.04588.x.

Pike, C.R., Roberts, A.P. & Verosub, K.L., 1999. Characterizing interactions in fine magnetic particle systems using first-order reversal curves, *J. appl. Phys.,* **85**(9), 6660–6667.

Roberts, A.P., Pike, C.R. & Verosub, K.L., 2000. First-order reversal curve diagrams: a new tool for characterizing the magnetic properties of natural samples, *J. geophys. Res.,* **105**(B12), 28461–28475.

Sahu, S. & Moskowitz, B.M., 1995. Thermal-dependence of magnetocrystalline anisotropy and magnetostriction constants of single-crystal $Fe_{2.4}$ $Ti_{0.61}$ O_4, *Geophys. Res. Lett.,* **22**(4), 449–452.

Sinton, J., Smaglik, S., Mahoney, J. & Macdonald, K., 1991. Magmatic processes at superfast spreading mid-ocean ridges: glass compositional variations along the East Pacific Rise, 13°–23° S, *J. geophys. Res.,* **96,** 6133–6156.

Stoner, E.C. & Wohlfarth, E.P., 1948. A mechanism of magnetic hysteresis in heterogeneous alloys, *Phil. Trans. R. Soc. Lond.,* **240**(826), 599–642.

Tauxe, L., 2010. *Essentials of Paleomagnetism,* p. 68, University of California Press, Berkeley, CA.

Tauxe, L., Constable, C., Stokking, L. & Badgley, C., 1990. Use of anisotropy to determine the origin of characteristic remanence in the Siwalik red beds of northern Pakistan, *J. geophys. Res.,* **95**(B4), 4391–4404.

Tauxe, L., Bertram, H.N. & Seberino, C., 2002. Physical interpretation of hysteresis loops: micromagnetic modeling of fine particle magnetite, *Geochem. Geophys. Geosyst.,* **3**(10), doi:10.1029/2001GC000241.

Wohlfarth, E.P., 1958. Relations between different modes of acquisition of the remanent magnetization of ferromagnetic particles, *J. appl. Phys.,* **29**(3), 595–595.